Beilstein-Institut

Experimental Standard Conditions of Enzyme Characterizations,
September 13th – 16th, 2009, Rüdesheim/Rhein, Germany

Understanding Enzymes as Reporters or Targets in Assays Using Quantitative High-throughput Screening (qHTS)

Douglas S. Auld*, Natasha Thorne, Matthew B. Boxer, Noel Southall, Min Shen, Craig J. Thomas and James Inglese

NIH Chemical Genomics Center, National Institutes of Health, Bethesda, MD 20892 – 3370, U.S.A.

E-Mail: *dauld@mail.nih.gov

Received: 5th January 2010 / Published: 14th September 2010

Abstract

The U.S. National Institutes of Health Chemical Genomics Center (NCGC) has established a new screening paradigm, quantitative high-throughput screening (qHTS), wherein concentration-response curves (CRCs) are rapidly recorded on large compound collections (> 300,000). The data is automatically fit to the Hill equation and the CRCs are subjected to a classification scheme. This approach reduces false positive and negative rates compared to the traditional screening approaches where only a single concentration is tested and provides a pharmacological database that can be used to construct large-scale bioactivity profiles. We demonstrate how this approach was used to examine a coupled enzyme assay where the production of ATP by human pyruvate kinase M2 (PykM2) was coupled to the ATP-dependent bioluminescent enzyme, firefly luciferase (FLuc), to produce a luminescent signal. This identified chemical probes which specifically activate PykM2 while also providing a bioactivity profile of FLuc inhibitors. Examining the latter uncovered a counterintuitive phenomenon of great importance to compound discovery efforts wherein FLuc inhibitors specifically produce a non-specific luminescent response in cell-based assays.

Introduction

Screening of small molecule compound collections has been historically practiced within the pharmaceutical industry and only recently have high-throughput screening (HTS) methodologies been adopted to produce general research tools which can be applied to uncover mechanisms of biological function [1, 2]. The term ''chemical biology'' is now widely used in reference to identifying compounds that act as positive or negative regulators of individual gene products or signalling pathways in an effort to further the understanding of complex biological networks [3, 4]. In 2003, the U.S. National Institutes of Health (NIH) as part of the NIH Roadmap for Medical Research (http://nihroadmap.nih.gov), started the Molecular Libraries Initiative (MLI) to provide industrial-scale HTS technologies and chemical probes for basic research [5 – 7] (for more information see: mli.nih.gov). Importantly, both chemical and biological assay information is now freely accessible through the creation of the PubChem database [8] (http://pubchem.ncbi.nlm.nih.gov).

At the NIH Chemical Genomics Center (NCGC), we have endeavored to bring the expertise from both the pharmaceutical and academic communities together to enable the discovery of chemical probes and to create robust datasets that can be mined for structure-activity relationships (SAR). Compound discovery in either chemical biology or drug discovery starts with a single experiment wherein a bioassay is screened against a diverse compound collection. This experiment is critical to the entire discovery process as the results will often set the compass which guides all subsequent efforts. To provide the optimum starting point, as well as to capitalize on the most thorough use of sophisticated assays that may have taken years to develop, we have developed a novel screening paradigm, termed quantitative HTS (qHTS), where chemical libraries of about 300,000 compounds are screened at multiple concentrations so that concentration-response curves (CRCs) are measured for every compound. This provides a high quality dataset that can be used to drive chemical optimization efforts and allows construction of pharmacological databases that can be mined for bioactivity relationships. Here we present an overview of the challenges that had to be overcome to develop and implement qHTS in addition to presenting a case study of a coupled enzyme assay to highlight what has been learned while implementing this approach.

Overview of the Construction and Classification of Large Concentration-response-based Datasets

Physical construction of a compound dilution series can employ two general strategies: One where the compounds are titrated within the same microtiter plate to create a ''horizontal'' intra-plate dilution series and another where the compound dilution series is constructed in a ''vertical'' inter-plate manner by diluting the compound between successive microtiter plates. We selected a vertical inter-plate dilution method at the NCGC for qHTS operations [9]. In this case, plates are assayed in a manner where the first plate contains the lowest concentration of a set of compounds while subsequent plates contain the same compounds in

the same well locations, but at successively increasing concentrations (Fig. 1a). This approach to large-scale concentration-series plating offers several advantages to the intra-plate method which include increased flexibility in plate usage for screening a wide variety of assay systems, and ease and speed of plate preparation [9, 10]. The vertically-developed dilution method allows one to choose between testing multiple concentrations or limiting the concentration range as necessitated by factors such as target concentration, assay sensitivity, and reagent cost (Fig. 1b).

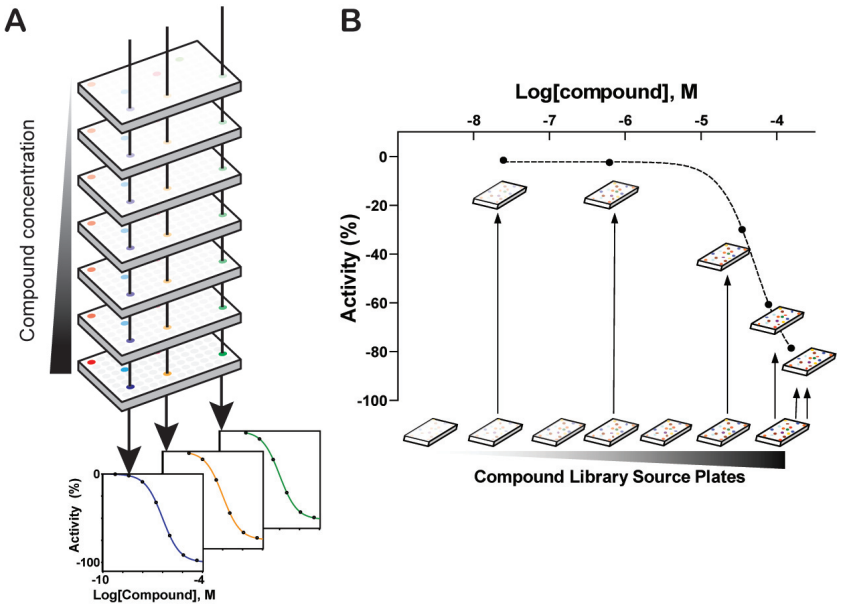

Figure 1. Construction, flexibility and customization of CRCs with qHTS. (A) Microtiter plates containing compounds in DMSO are diluted serially into DMSO to create daughter plates that contain the same compounds at the equivalent positions but at successively lower concentrations. Typically, five-fold dilutions are used for a seven point dilution series or dilutions at a fold = $\sqrt{5}$ are used to create a 14 point dilution series over the same concentration range. Shown at the bottom are CRCs obtained from the data collected from assay plates that each received 20 nL of compound solution. (B) Construction of asymmetric titration series using a set of dilution plates. Arrows represent the 20 nL transfer of compound solution from the source plates (below) to the assay plates (above). In this example, the highest concentration point is customized to contain a two-fold higher compound concentration which is achieved by a double transfer (dual arrows) from the highest concentration source plate. Adopted from Yasgar *et al.*, 2008 [9].

Management of the 350k compound archive for qHTS at the NCGC requires processes to acquire, register, and track > 2 million sample wells, an undertaking comparable to a large pharmaceutical company [11]. The operations for this endeavor which include analytical chemistry, engineering, and software development have been described elsewhere [1, 9, 12, 13]. To minimize the cost of the compound screen and time on the robotic system, we

employ miniaturized assay volumes (between 2 and 10 μL volumes) in 1,536-well microtiter plates. A typical assay protocol involves dispensing a reagent into a 1,536-well assay plate, transferring 20 nL of a DMSO compound solution to the assay plate, transfering appropriate controls to the assay plate (128 wells are reserved for controls on every microtiter plate), incubation of the assay components, and measurement of activity. Following measurement, the raw data is normalized to controls, corrected for systematic errors (due to, for example, liquid dispensing), and the quality of the data is checked by calculating the coefficient of variation (CV) between sample wells, signal to background ratio, Z-factor, and the reproducibility of potency values if control titrations were used [1, 12, 14, 15]. This provides the initial dataset used for subsequent fitting of concentration-response curves (CRCs).

Indeed one of the greatest challenges we faced in implementing the qHTS method was a means to rapidly and automatically fit CRCs to the > 2 million data points generated from a single qHTS experiment. Commercial software packages lacked the ability to fit hundreds of thousands of CRCs. Even more difficult was finding a strategy to rank the CRCs in terms of curve-fit quality and compare the pharmacological responses between CRCs. To solve this, in-house software has been developed that includes identification of outlier data points, one of the largest impediments to automated curve-fitting. Commonly, outlier detection involves determining if a datapoint is significantly different (*e.g.* 3 s.d.) from the mean value. However, in concentration-response data the mean has not been determined and the mean is in fact exactly what is being fitted. Therefore, we developed a robust automated curve-fitting algorithm which results in a curve fit using a four parameter Hill equation [16, 17]:

$$y = S_0 + \frac{S_{\inf} - S_0}{1 + \left(10^{\log AC_{50} - x}\right)^n}$$

Where S_0 is the activity at zero compound concentration, S_{inf} is the activity at infinite compound concentration, AC_{50} is the concentration at which the activity reaches 50% of maximal level (either activating or inhibiting). x is the tested concentration range, y yields the observed response, and n is the Hill coefficient, the slope at the AC_{50} [18]. The curve-fitting employs line interpolation based on connecting datapoints or from an expected value (*e.g.* the basal activity should be close to zero), as well as iterative curve-fitting where datapoints are masked if excluding these yields a better fit to the data. To estimate the quality of the fit to the model we use R^2, defined as

$$R^2 = 1.0 - SS_{(\text{Hill fit})}/SS_{(\text{constant fit})}$$

SS is the sum-of-square of the vertical distances of the points from the curve (Hill fit) or a straight line (constant fit). In this approach values of the four parameters are exhaustively sampled to find the combination having the best R^2. For this purpose, the Hill slope is constrained to values between 0.3 and 5.0, as we have found that values > 5.0 have little

effect on the curve fit given the number of concentration points tested in qHTS. A version of the curve-fitting software is freely available at http://www.ncgc.nih.gov/resources/software.html (and see [19] for a more detailed description).

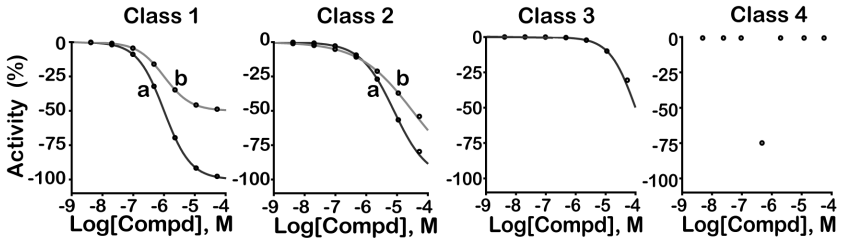

Figure 2. CRC classification scheme. Class 1 curves display two asymptotes, an inflection point, and $R^2 \geq 0.9$; subclasses 1a versus 1b are differentiated by full (> 80%) versus partial (≤ 80%) response. Class 1a curves demonstrate high activity. Class 2 curves display a single left-hand asymptote and inflection point; subclasses 2a and 2b are differentiated by a maximum response and R^2 with either > 80% and > 0.9 or < 80% and < 0.9, respectively. Class 3 curves have a single left-hand asymptote, no inflection point, and a response > 3 s.d. the mean activity of the sample field; hence they are lower confidence curves. Class 4 defines those samples without any concentration–response relationship; thus they are inactive. Adopted from Shukla *et al.* 2009 [20].

The next issue to be overcome once the CRCs are obtained is a strategy to assess the quality of the curve-fit to the data as well as to compare the pharmacological parameters (*e.g.* potency and efficacy of the response) obtained between active CRCs. Common statistical tests such as the F-test have not proven useful to rank CRCs and the values of these parameters do not reflect the nature of the pharmacological response [19]. To help address these issues we developed a CRC classification scheme shown in Figure 2 [12, 20]. Classification of the CRCs in this manner provides an easily understood number reflecting both the quality of the curve-fit to the data along with information about the pharmacological response. Once the CRC classification numbers are assigned these can be used to cluster structurally related compounds to determine which of these are associated with high quality CRCs as well as those with less efficacious/potent CRCs and inactive compounds. The SAR obtained from such analysis can be immediately employed to optimize chemical probes for the intended target or to construct robust bioactivity profiles that can reveal unexpected hidden phenotypes associated with a chemical series. We illustrate both of these approaches below by examining a simple coupled enzyme assay with qHTS.

Application of qHTS to Identify Chemical Probes of Human Pyruvate Kinase

Pyruvate kinase (Pyk; EC 2.7.1.40) is an allosterically regulated enzyme that functions in the final step of glycolysis to convert one molecule of ADP and phosphoenol pyruvate (PEP) to ATP and pyruvate. In cells, this reaction proceeds far from its equilibrium and PyK has one of the lowest V_{max} values among glycolytic enzymes making this one of the rate-determining steps in glycolysis. Metabolic regulatory steps catalyzed by such allosteric enzymes are responsible for the homeostasis of metabolites [21]. In cancer cells homeostasis is shifted to support rapid cellular proliferation, an abnormal state of flux for mature tissue cells [22].

Otto Warburg was first to note that cancer cells show aberrant glycolysis, producing lactate even in the presence of oxygen [23, 24]. This abnormal metabolic phenotype has become known as the ''Warburg effect'' (Fig. 3A) and is thought to be due at least in part to over expression of specific enzymes such as lactate dehydrogenase and the expression of a tumor specific isozyme of pyruvate kinase – PyKM2 [25 – 27].

Humans have four isozymes of PyK expressed from two genes which undergo alternative splicing [28, 29]. The Pyk L/R gene produces the liver (PyKL) and red blood cell (PyKR) forms. The pre-mRNA from the Pyk M gene is alternatively spliced in a region that encodes the allosteric activation loop of PyK (Fig. 3B) to produce the M1 isozyme (PyKM1). PyKM1 is found in most normal adult tissues and this alternative splicing results in this isoform being insensitive to regulation by fructose-1,6-bis-phosphate (FBP). In contrast, the PyKM2 isoform is activated by FBP and is only normally expressed in fetal tissue but also shows aberrant expression in tumor cells [28, 30, 31]. All tumors and cancer cell lines studied to date exhibit exclusive expression of the PyKM2 isozyme [32, 33].

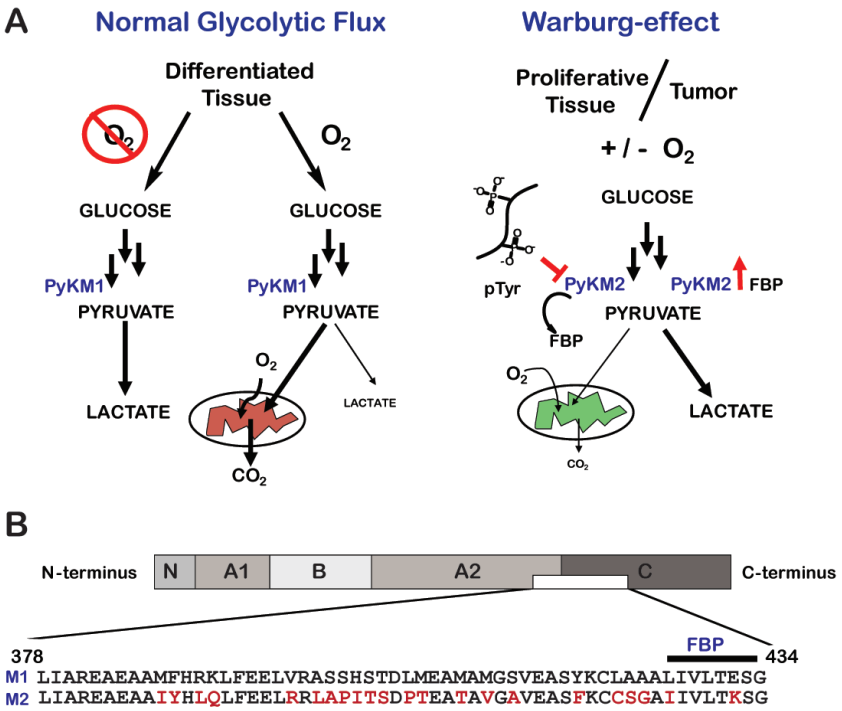

Figure 3. The Warburg effect and differential regulation of PykM1/M2. (A) Left, shows the normal state of glycolytic flux where PyKM1 is expressed in many differentiated healthy tissue types. In aerobic environments glucose is metabolized to pyruvate which is utilized by the Krebs cycle within the mitochondria; or in anaerobic environments glucose is converted to lactate. Right, illustrates the Warburg effect associated with cancer cells where glucose is converted to lactate under either aerobic or anaerobic environments. This abnormal metabolism is in part due to the expression of tumor specific enzymes such as PyKM2 which is allosterically regulated by FBP and phospho-polypeptides (pTyr) which are abundant in cancer cells from growth factor signaling pathways. The binding of pTyr is thought to down-regulate PyKM2 activity by removing the allosteric activator FBP, resulting in a build-up of glycoltyic metabolites that feed proliferation. (B) The PyKM1 and M2 isoforms arise from the M gene through alternative splicing of exons 9 and 10 located at the interface of the A and C domains. These exons encode a stretch of 56 amino acids and splicing results in amino acid differences between the two isoforms (highlighted in red for PyKM2) which includes a portion of the FBP binding pocket.

In cancer cells, the dimeric form of PyKM2 has low activity, but upon binding of FBP to its activation loop the tetrameric form of the enzyme is stabilized, leading to activation by increasing the enzyme's affinity for PEP [30, 33]. Low activity of PyKM2 in cancer cells acts to shunt key glycolytic metabolites toward biosynthetic pathways, a necessary requirement for rapidly proliferating cells such as those found in fetal tissues and tumors. Additionally, recent work has shown that replacement of PyKM2 with PyKM1 in cancer cells

relieves the Warburg effect and restores a metabolic phenotype characteristic of normal cells [26]. The lung carcinoma line, H1299, when engineered to express only PyKM1 showed delayed tumor formation in nude mouse xenografts [26]. Recently, a link between growth factor signaling and PyKM2 has been shown where phosphotyrosine peptides (prevalent in cancer cells from growth factor signaling pathways) bind to PykM2 near the allosteric activation loop. Phosphotyrosine peptide binding to PykM2 results in release of FBP from the enzyme leading to further down-regulation of this critical step in glycolysis (Fig. 3A) [27]. Therefore, one approach to anti-cancer therapy would be identifying compounds that activate human PyKM2 to PyKM1 levels, which should help restore normal metabolism, shifting the glycolytic flux back toward the demand for energy rather than biosynthesis.

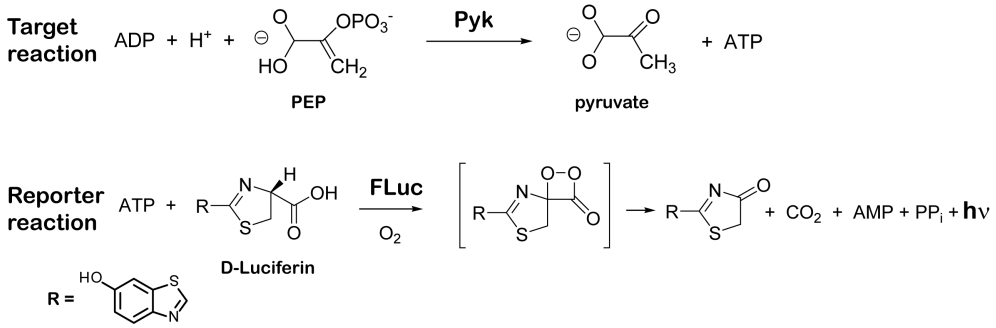

Figure 4. The pyruvate kinase-FLuc coupled assay. Three μL of substrate mix (at r.t.) in assay buffer (50 mM imidazole pH 7.2, 50 mM KCl, 7 mM $MgCl_2$, 0.01% Tween 20, 0.05% BSA) was dispensed into Kalypsys white solid bottom 1,536 well microtiter plates using a bottle-valve solenoid-based dispenser (Kalypsys). The final concentrations of substrates in the assay were 0.1 mM ADP and 0.5 mM PEP. 23 nL of compound were delivered with a 1,536-pin array tool [47] and 1 μL of enzyme mix in assay buffer (final concentration, 0.1 nM PyKM2, 50 mM imidazole pH 7.2, 0.05% BSA, 4 °C) was added. Microtiter plates were incubated at r.t. for 1 hour and 2 uL of luciferase detection mix (Kinase-Glo, Promega [48] at 4 °C protected from light) was added and luminescence was read with a ViewLux (Perkin Elmer) using a 5 second exposure/plate.

The coupled assay shown in Figure 4 was designed to find both inhibitors and activators of PyKM2 and was applied to qHTS of about 300k compounds in the Molecular Libraries Small Molecule Repository (MLSMR). The assay of ca. 2.56 million sample wells performed well with Z-factors of 0.78 ± 0.07 and CVs of 10 ± 3%. This identified 777 high quality activating CRCs (0.27% of the library; Fig. 5). Inhibitory CRCs were also found (~0.02% high quality CRCs), but most of these were subsequently found to be inhibitors of the luciferase coupling enzyme (see below). The primary qHTS data is available in PubChem (AIDs: 1631 and 1634).

A

Activity	Distribution	CRC Class					
		1a	1b	2a	2b	3	4
Activation	# Cmpds.	134	318	325	1541	2094	
	% library	0.05	0.11	0.11	0.55	0.74	276,309
Inhibition	# Cmpd	4	25	31	582	983	97.73%
	% library	0.00	0.01	0.01	0.21	0.35	

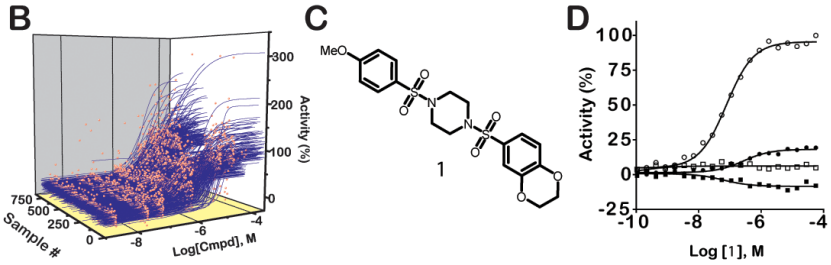

Figure 5. Summary of the qHTS against PyKM2.
(A) Distribution of activity by CRC class. (B) CRC's for actives from the qHTS associated with CRC classes 1a, 1b and 2a showing potency and maximum response. (C) Chemical structure of the substituted N,N′-diarylsulfonamide NCGC00030335 (**1**). (D) Selectivity assessment for **1** versus PyKM2 (open circles), PyKM1 (filled squares), PyKL (open squares), and PyKR (filled circles).

To define the SAR between compounds showing activation of PyKM2 activity we clustered structures showing high quality CRCs by structurally similarity (Fig 6). This identified a series of activators with a common substituted N,N'-diarylsulfonamide core structure. We next used this core structure to query the entire qHTS dataset to identify related structures associated with weaker CRCs or inactive compounds to allow a complete SAR from the qHTS to be developed. One of the more potent activators in this chemical series was compound **1** (Fig. 5).

After resynthesis and confirmation of chemical structure and purity, we examined the mode of action of **1** against PyKM2 through analysis of the compound's effect on the steady-state kinetics of PEP and ADP. Kinetic assays were carried out at 25 °C with 10 nM PyKM2 using [KCl] = 200 mM, [$MgCl_2$] = 15 mM, and with either [ADP] or [PEP] = 4.0 mM through the measurement of pyruvate in a lactate dehydrogenase coupled assay [34]. As discussed, FBP is known to allosterically activate PyKM2 through induction of an enzyme state with a high affinity for PEP. Consistent with these observations, in the absence of activator, we found that PyKM2 shows low affinity for PEP ($S_{0.5}$ ~ 1.5 mM). We found that in the presence of either 10 μM **1** or FBP the K_M for PEP decreased nearly 10-fold to 0.26 ± 0.08 mM or 0.1 ± 0.02 mM, respectively, with lesser effects on V_{max} (values of 245 pmols/min with or without FBP and 265 pmols/min with **1**) [34]. The addition of excess PEP abolishes the activation of PyKM2 by **1** or FBP. However, varying the concentration of ADP in the presence and absence of **1** shows that the steady-state kinetics for this substrate

are not significantly affected (K_M for ADP = 0.1 mM in either condition). Akin to what has been observed for FBP, our primary lead NCGC00030335 (**1**) lowered the K_M for PEP but had no affect on the steady-state kinetics of the ADP reaction [34].

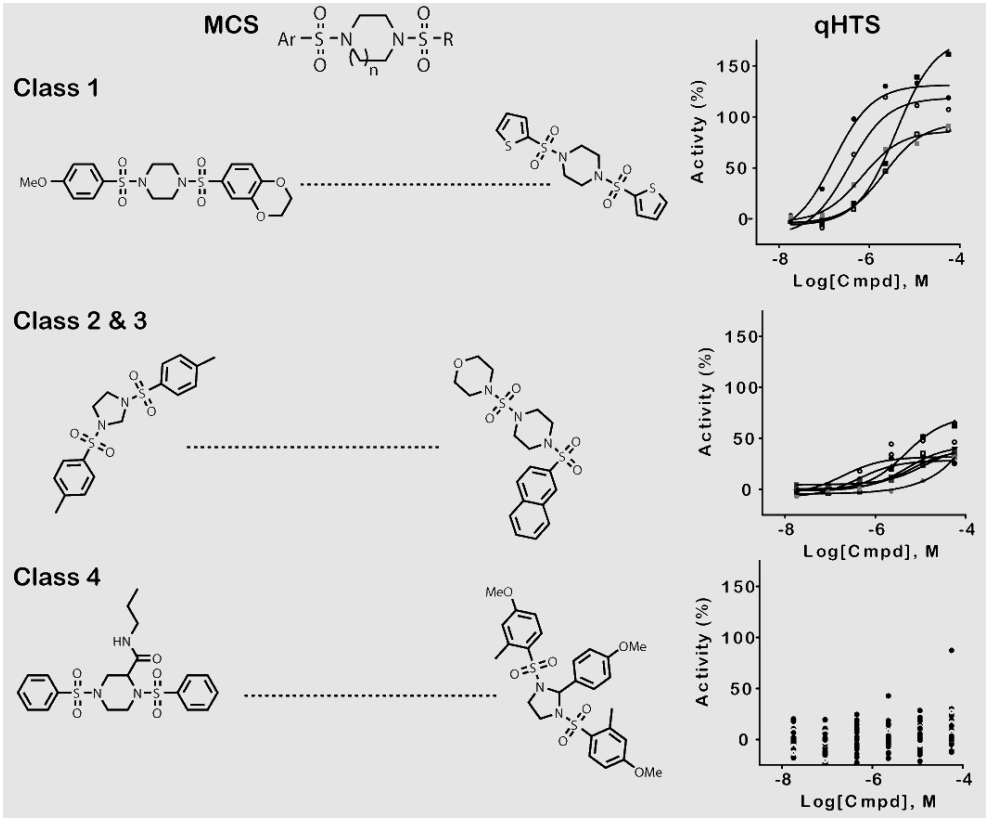

Figure 6. SAR development using primary qHTS data. In the example shown, structures associated with high quality CRCs were subjected to hierarchical clustering using Leadscope fingerprints to define a maximal common substructure (MCS). This MCS can then be used to identify similar structures associated with lower confidence CRCs or that are inactive. Example structures for the PyKM2 activator series and CRCs from the qHTS are shown.

This provided an informative dataset to initiate chemical optimization of these leads. Synthesis of nearly 300 analogs refined the SAR for this chemical series [34]. While the potency of the series was generally good (< 1 μM), the lack of aqueous solubility was a major liability for these compounds. Many analogs had solubility levels below detectable limits (e. g. **2** in Table 1). The solubility of **3** containing a seven-member ring system showed low values of 5.6 μg/mL (2.7 μM; Table 1). With an understanding of the SAR we were able to design and synthesize numerous analogues incorporating more soluble functional groups which maintained potency (**4 – 8,** Table 1; including pyridines, anilines and N-acetyl ani-

lines). These compounds are currently being tested in cell-based assays for anti-proliferative activity and should be useful chemical probes to study the role of the Warburg effect in tumor models.

Table 1. SAR of selected *N,N'*-diarylsulfonamides including solubility assessment.

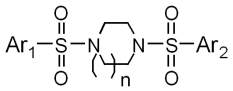

#	n	Ar_1	Ar_2	*hPK, M2 AC_{50} (μM)*[a]	*hPK, M2 Max. Res.*[b]	Solubility[c] *(μM)*	Solubility[c] *(μg/mL)*
2	1	2,6-difluorobenzene	6-(2,3-dihydrobenzo[*b*][1,4]dioxine)	0.065	94	< 1.1	< 0.5
3	2	2,6-difluorobenzene	6-(2,3 -dihydrobenzo[*b*][1,4]dioxine)	0.866	120	5.6	2.7
4	1	3-aniline	2,6- difluoro-4-methoxybenzene	0.023	87	< 0.7	< 0.4
5	1	3-aniline	6-(2,3 -dihydrobenzo[*b*][1,4]dioxine)	0.041	82	7.3	4.1
6	1	3-aniline	2,6-difluorobenzene	0.092	82	5.7	3.0
7	2	3-aniline	2,6-difluoro-4-methoxybenzene	0.206	93	26.3	15.1
8	2	3-aniline	6-(2,3-dihydrobenzo[*b*][l,4]dioxine)	0.033	89	51.2	29.0

[a]AC 50 values were determined utilizing the luminescent pyruvate kinase-luciferase coupled assay and the data represents the results from three separate experiments. [b]Max. Res. value represents the % activation at 57 μM of compound. [c]kinetic solubility analysis was performed by Analiza Inc. and are based upon quantitative nitrogen detection as described (www.analiza.com). The data represents results from three separate experiments with an average intra-assay %CV of 4.5%.

Application qHTS to Reveal an Unexpected Cellular Phenotype Associated with Firefly Luciferase Inhibitors

Enzymes are widely employed as reporters for biological assays aimed at screening large chemical libraries using HTS systems. The commercialization of firefly luciferase (FLuc) assay reagents has lead to widespread use of this enzyme. However, failure to appreciate the underlying enzymology can lead to a misuse of this powerful assay technology resulting in misinterpreted results. In drug discovery the HTS assay often sets the course of action for a development program that can take 10 to 15 years to transpire at a cost of US$ 800 M. Initiating this process with well-considered leads may significantly improve the efficiency of drug discovery. Therefore, at the NCGC we have endeavored to understand the mechanisms underlying assay interference, a major impediment to the identification of quality leads. The FLuc enzyme is one of the most common reporter enzymes used in bioassays [35] and we sought to determine how this enzyme's activity is modulated by small molecules found in typical HTS compound collections.

Using qHTS we determined the concentration-response behavior for > 70,000 compounds in the MLSMR against the ATP-dependent luciferase from the firefly *Photinus pyralis* (FLuc; PubChem AID: 411; EC 1.13.12.7). Approximately 3% of the library showed inhibitory

activity while none of the compounds caused activation of enzyme activity. Given that the activity relevant to the target being explored in a typical HTS is ~0.01 – 0.1%, this level of inhibition is highly significant and will easily confound the analysis of actives from a screen if steps are not taken to address this "off-target" activity.

Through examination of this profile we were able to define the SAR for prominent luciferase inhibitor series [35]. We identified several structural classes of inhibitors which included compounds showing structural similarity to the benzthiazole core of the substrate D-luciferin. Scaffolds likely to mimic the D-luciferin substrate were often found to be competitive with D-luciferin, but not ATP (Fig. 7a), while others such as those containing a quinoline core were found to be ATP competitive as well (Fig. 7b). Compounds showing no structural similarity to either ATP or D-luciferin but possessing potent inhibitory activity (such as a series of 3,5-diaryl oxadiazoles) were also identified (Fig. 7c).

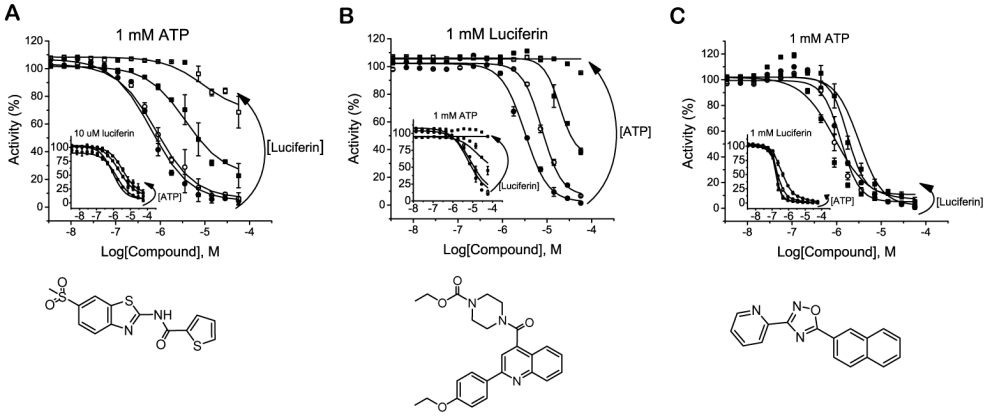

Figure 7. Representative luciferase inhibtors from the FLuc qHTS. Shown is the dependence of inhibition on substrate concentration for three representative compounds. Luciferin or ATP was varied at (●) 1 μM, (O) 10 μM, (■) 100 μM, and (□) 1000 μM. (A) Substrate variation data for a benzthiazole representing a compound likely to mimic the D-luciferin substrate. The graph shows that inhibition can be relieved upon increasing the luciferin concentration, and the inset graph shows that ATP variation has little effect on the inhibition (holding the luciferin concentration constant at 10 μM, approximately the K_M). (B) Substrate variation data for a representative quinoline. The graph shows that inhibition can be relieved when either the ATP or the luciferin concentration (inset graph) is increased. (C) Substrate variation data for a 3,5-diaryl oxadiazole. The graph shows that the inhibition remains relatively constant when varying either the luciferin or the ATP concentration (inset graph). Adapted from [35].

Our profile used a cell-free system with purified FLuc to define inhibitors. However, FLuc is commonly used in cell-based reporter-gene assays because the luminescent response provides a sensitive assay signal. Due to the relatively short protein half-life of FLuc this reporter can be used to measure dynamic responses in gene regulation where either increases

or decreases in luciferase activity are measured [36]. Enzymes can be stabilized by inhibitors [37] when an E•I complex is more resistant to degradation than the free enzyme. For this to occur, the reporter enzyme (E) expressed in a cell must bind to a cell-penetrating inhibitor (I) leading to an E•I complex within the cells that stabilizes the enzyme. This may occur, for example, due to a conformational change upon inhibitor binding that stabilizes the enzyme from degradation. Therefore, assuming no effect due to transcription or translation, we would expect the total amount of active enzyme (E) at any time to depend on the concentration of E•I, which, itself is dependent on the affinity of the complex within the cells. The degradation of the free enzyme (E_f) and E•I can be shown as:

$$E* \underset{\leftarrow}{\overset{k_2}{}} E \cdot I \overset{K_I}{\underset{\leftrightarrow}{}} + E_f \overset{k_1}{\underset{\rightarrow}{}} E*$$

Where E* is degraded inactive enzyme and the rate of degradation is

$$-\frac{dE}{dt} = k_1\left[E_f\right] + k_2[E \cdot I](k2 < k1)$$

The amount of intact active enzyme (E) produced will be modulated by term ($1+I/K_I$). When the ratio of I to K_I is high, the slower degrading E•I complex is maximized so that degradation of the enzyme is minimized. This simple model predicts that at different concentrations of I the amount of active enzyme available will follow a CRC with an apparent EC_{50} that parallels the affinity of inhibitor for the enzyme (K_I; Fig. 8A). However, the final apparent pharmacology that is observed in the assay will depend on the sum of two opposing inhibitor responses: the positive increase in enzyme levels due to the stabilization by the inhibitor in the cells and the opposing inhibitory effect on the enzyme reaction during the detection step where excess substrates are added. Depending on the mode of action of the inhibitor (*e.g.* reversible or irreversible, competitive or noncompetitive) and the configuration of the assay different cases are possible and these are illustrated in Figure 8 [38]. Inhibitors that are not completely removed by the detection reagents can show bell-shaped CRCs, a phenomenon that is typically attributed to cytotoxicity in cell-based assays although reporter inhibition can lead to the same response.

We have experimentally demonstrated that inhibitor-based stabilization of FLuc occurs for representative chemotypes from FLuc our inhibitor profiling efforts [35, 39]. We measured the CRCs for luciferase activity before and after treating cells with cycloheximide for 24 hours. The same compounds were also measured in an assay using purified FLuc and K_M levels of substrates to confirm the inhibitory effect of these compounds. In these experiments, we observed apparent activation of the luciferase signal upon addition of a reporter-gene detection cocktail containing excess luciferase substrates which we found can occur at concentration ranges typically used in HTS (1 – 10 μM; Fig. 8C). Examination of the stability of the signal after cycloheximide treatment showed a slower rate of activity decay from samples treated with inhibitor compared to samples without inhibitor [39]. Plots of the relative amount of luciferase activity remaining after a 24 h treatment with cycloheximide

(Fig. 8C, red line) showed a CRC that mirrored the inhibition against the purified enzyme. These parallel but opposite responses are expected based on stabilization of an E●I complex, where the potency for activation response within cells mirrors the inhibition potency against the purified enzyme (as described above) and strongly supports that increased FLuc activity is due to inhibitor based-stabilization of the FLuc enzyme.

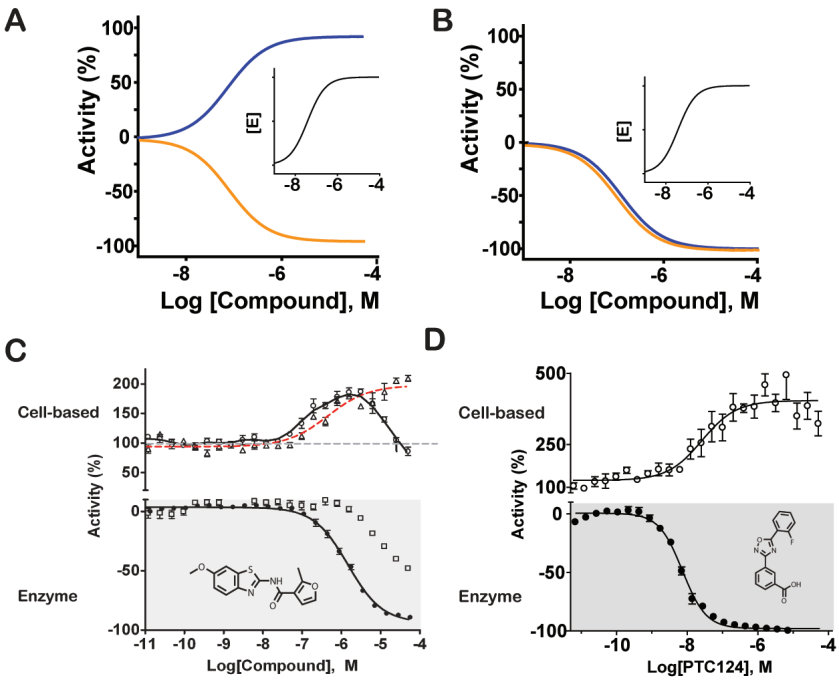

Figure 8. Post-translational inhibitor-based stabilization of FLuc in cell-based assays. Shown is what should be theoretically observed for reporter activity in the cell-based assays (blue lines) and the activity against the reporter enzyme determined in a biochemical assay where substrates are at low concentrations (e.g.,~ K_M; orange lines). Insets illustrate the increase in intracellular enzyme concentration in the assay as a result of inhibitor-based stabilization. (A) If the cells are treated with a reversible competitive inhibitor of luciferase, after interaction and stabilization of the luciferase protein (inset), the compound can be competed off the luciferase enzyme after cell lysis by the addition of a detection reagent containing excess substrates. In this case, apparent activation is observed in the cell-based assay (blue curve) that mirrors the inhibition of the reporter enzyme in a cell-free, biochemical assay. Alternatively, activity from reversible noncompetitive inhibitors may be detected by removal of the inhibitor through cell wash steps prior to detection. (B) If the cells are treated with a compound that acts as an irreversible or a noncompetitive inhibitor of the luciferase enzyme (orange curve) where the inhibitor is not removed before detection, stabilization of the reporter enzyme still occurs (inset), but in this scenario inhibition is likely observed (blue curve) because the inhibitor is not displaced from the enzyme during detection. Adopted from ref [38]. (C) More complex apparent activation behavior such as bell-shaped concentration–response curves may also occur as illustrated

here for luciferase activity measured from HEK293 cells expressing FLuc and treated with compound for 24 h (top graph) (O, black fitted line) or the remaining luciferase activity following 24-h treatment with cycloheximide (red fitted line). Bottom graphs depict the cell-free luciferase activity determined using purified luciferase assayed with a commercial reporter gene detection cocktail (SteadyGlo™, Promega □) or using K_M concentrations of luciferase substrates (●). See [39]. (D) (Upper) FLuc activity from Grip-Tite 293 cells transfected with the pFLuc190^{UGA} construct and treated with PTC 124 for 24 h (PTC 124; open circles) shows concentration-dependent activation. (Lower) Activity of purified FLuc enzyme (with K_M concentrations of substrates) shows concentration-dependent inhibition with compound treatment (filled circles). In this case, the inhibitor was removed from the cells by wash steps prior to detection (see [38] for further details).

To examine the prevalence of this phenomenon among HTS assays using FLuc, we examined the enrichment of luciferase inhibitors in 100 FLuc assays found in PubChem (Fig. 9). As our luciferase qHTS identified a frequency of luciferase inhibitors of 3%, active sets within PubChem containing only 3% luciferase inhibitors would not be considered enriched in luciferase inhibitors. However, an HTS active set found to contain, for example, 30% luciferase inhibitors is enriched 10-fold. As anticipated, we found an enrichment of luciferase inhibitors in luciferase-based assays designed to identify compounds acting as inhibitors in either biochemical or cell-based assay formats (yellow and blue bars in Figure 9, respectively). However, reporter-gene assays targeting an increase in luciferase activity also displayed a similar enrichment of luciferase inhibitors within active data sets (Fig. 9, orange bar). In contrast, no enrichment in luciferase inhibitors was observed for reporter-gene assays employing unrelated enzymes such as β-lactamase (EC 3.5.2.6), non-enzymatic reporters such as GFP, or in other assay formats using fluorescence or chemiluminescent detection strategies (Fig. 9, light grey bar). Therefore, the prevalence of luciferase inhibitors within PubChem (which represents a typical diverse screening collection) and their enrichment in luciferase reporter-gene assays aimed at activation, suggests that inhibitor-mediated reporter stabilization is a common artifact associated with cell-based assay formats using FLuc.

One of the most potent and prominent chemical series of FLuc inhibitors was contained within a subset of 3,5-diaryl-oxadiazoles. A 3,5-diaryl-oxadiazole that has received significant attention due to its purported activity as a nonsense codon suppressor and is in clinical trials for DMD and CF is PTC 124 (Fig. 8D, [40 – 42]. PTC 124 was identified as a compound that apparently increased the frequency of read-through of a premature nonsense mutation in a FLuc gene [42]. The FLuc cell-based assay used to test compounds for this activity relied on the detection of increased luciferase activity, presumably due to increased translation of full-length FLuc protein as a result of nonsense codon suppression activity by the small molecule. In the initial characterization of PTC 124, FLuc activity was shown to increase while FLuc mRNA levels were unchanged in the presence of PTC 124 [42]. Though consistent with this data, the possibility of post-translational reporter stabilization was not investigated. Therefore, we examined if the activity of PTC 124 and other 3,5-diaryl-oxa-

diazole analogs was attributed to post-translational stabilization of the FLuc reporter itself [38]. We found that PTC 124 and related analogs, as well as structurally unrelated FLuc inhibitors, all showed similar levels of activation in a FLuc-dependent reporter assay of nonsense codon suppression where the apparent activation paralleled inhibition against the purified FLuc enzyme, consistent with formation of a stable cellular E●I complex (for example CRCs for PTC 124 see Figure 8D, and see [38]). Further, we found no apparent nonsense codon suppression activity for PTC 124 when employing an orthogonal luminescent reporter enzyme *Renilla reniformis* luciferase (RLuc; EC 1.13.12.5) in an analogous assay. RLuc enzymatic activity was refractory to inhibition by PTC 124 and structurally related analogs [38]. Based on these lines of evidence we conclude that the initial discovery of PTC 124 was biased by post-translational inhibitor-based reporter stabilization.

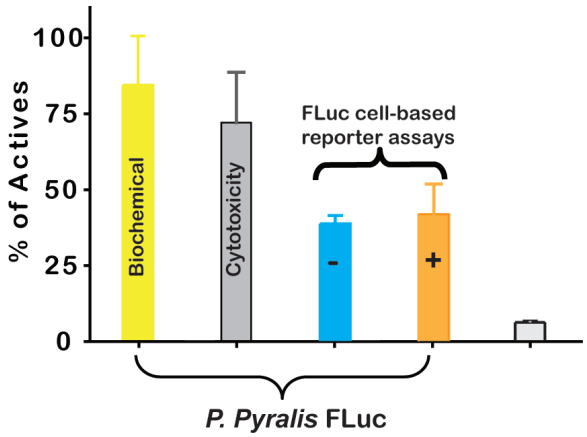

Figure 9. Percentage of luciferase inhibitors within hits from 100 PubChem assays. The PubChem active list from each assay was compared to the luciferase qHTS activity and all compounds showing inhibitory CRCs in the luciferase assay were used to calculate the percentage. Bars show the average and s.d. for the percentage of FLuc inhibitors found in each assay type. Data for figure is taken from from ref [39]. Yellow bar, *P. pyralis* luciferase-based biochemical assays (n = 6); Grey bar, cytotoxicity assays using *P. pyralis* (Perkin Elmer detection reagent; n = 4); blue bar, cell-based reporter-gene assays scored for inhibition (n = 9); Orange bar, cell-based reporter-gene assays scored for activation (n = 11); light grey bar other assay types including cell-based reporter-gene assays using β-lactamase, FRET-based assays, absorbance-based assays, and fluorescent-based assays (n = 70).

Our study of luciferase inhibitors has provided essential guidance for application of this enzyme in assay development and HTS [43]. In general, whether or not apparent activation is detected will depend on how much E●I is formed within the cells that results in stabilization and how efficiently the inhibitor is competed off in the presence of detection reagents [38, 44, 45]. Given these factors, this effect will be most commonly observed in assays which show an initially low basal level of luciferase expression and where a competitive inhibitor functions to stabilize the reporter. Use of commercial detection reagents containing

excess FLuc substrates/co-factors readily removes the competitive inhibitor to allow detection of FLuc activity which is easily misinterpreted as apparent activation of the reporter gene.

We recommend a few counter-screens to detect if inhibitor-based reporter stabilization is operating in FLuc cell-based assays. One such counter-screen is a purified FLuc enzyme assay using defined (K_M levels) of substrates to properly measure inhibition. An attenuated luciferase expression system, independent of the biology being targeted, has been employed as a counter-screen [43]. In addition, a paired cell-based assay that is identical to the FLuc assay except that an unrelated reporter such as RLuc, GFP, or β-lactamase is substituted can be used. The use of such orthogonal assays [46], which are based on different reporters expressed in a common cell type, provide a method to detect if the compounds are showing genuine target-mediated activity.

Conclusion

Exploration of the PyKM2-FLuc coupled enzyme assay has lead to two important results. One is a chemical probe, a specific activator of the tumor specific isoform PyKM2, which will be useful in studying the Warburg effect in cancer and also serves as lead for anti-cancer drug development. The second is a compound profile which allowed us to connect luciferase inhibition to an unexpected phenotype where reporter inhibitors lead to apparent gene activation responses in FLuc cell-based assays. The counterintuitive finding that inhibitors of reporters can appear as activators in cell-based assays has not been widely appreciated although this type of ‘off-target’ response can bias the SAR of early phase compounds and misdirect subsequent efforts. These findings demonstrate the importance of basic research into HTS assay design and interpretation in which the basic principles of enzymology and pharmacology must be applied.

References

[1] Inglese, J., Auld, D.S. (2009). High Throughput Screening (HTS) Techniques: Overview of Applications in Chemical Biology. *In*: Wiley Encyclopedia of Chemical Biology, Volume 2, T. Begley, ed. (Hoboken: John Wiley & Sons, Inc.), pp. 260 – 274.

[2] Stockwell, B.R. (2004). Exploring biology with small organic molecules. *Nature* **432**: 846 – 854.
doi: http://dx.doi.org/10.1038/nature03196.

[3] Collins, F.S., Green, E.D., Guttmacher, A.E., and Guyer, M.S. (2003). A vision for the future of genomics research. *Nature* **422**:835 – 847.
doi: http://dx.doi.org/10.1038/nature01626.

[4] Spring, D.R. (2005). Chemical genetics to chemical genomics: small molecules offer big insights. *Chem. Soc. Rev.* **34**: 472 – 482.
doi: http://dx.doi.org/10.1039/b312875j.

[5] Austin, C.P., Brady, L.S., Insel, T.R., and Collins, F.S. (2004). NIH Molecular Libraries Initiative. *Science* **306**:1138 – 1139.
doi: http://dx.doi.org/10.1126/science.1105511.

[6] Lazo, J.S. (2006). Roadmap or roadkill: a pharmacologist's analysis of the NIH Molecular Libraries Initiative. *Mol. Interv.* **6**:240 – 243.
doi: http://dx.doi.org/10.1124/mi.6.5.1.

[7] Lazo, J.S., Brady, L.S., and Dingledine, R. (2007). Building a pharmacological lexicon: small molecule discovery in academia. *Mol. Pharmacol.* **72:**1 – 7.
doi: http://dx.doi.org/10.1124/mol.107.035113.

[8] Richard, A.M., Gold, L.S., and Nicklaus, M.C. (2006). Chemical structure indexing of toxicity data on the internet: moving toward a flat world. *Curr. Opin. Drug. Discov. Devel.* **9**:314 – 325.

[9] Yasgar, A., Shinn, P., Jadhav, A., Auld, D., Michael, S., Zheng, W., Austin, C.P., Inglese, J., and Simeonov, A. (2008). Compound Management for Quantitative High-Throughput Screening. *JALA Charlottesv Va* **13**:79 – 89.

[10] Auld, D., Inglese, J., Jadhav, A., Austin, C.P., Sittampalam, G.S., Montrose-Rafizadeh, C., McGee, J.E., and Iversen, P.W. (2007). HTS technologies to facilitate chemical genomics. *European Pharmaceutical Review* **12**:53 – 63.

[11] Archer, J.R. (2004). History, evolution, and trends in compound management for high throughput screening. *Assay Drug Dev. Technol.* **2**:675 – 681.
doi: http://dx.doi.org/10.1089/adt.2004.2.675.

[12] Inglese, J., Auld, D.S., Jadhav, A., Johnson, R.L., Simeonov, A., Yasgar, A., Zheng, W., and Austin, C.P. (2006). Quantitative high-throughput screening: A titration-based approach that efficiently identifies biological activities in large chemical libraries. *Proc. Natl. Acad. Sci. U.S.A.* **103**:11473 – 11478. doi: http://dx.doi.org/10.1073/pnas.0604348103.

[13] Michael, S., Auld, D., Klumpp, C., Jadhav, A., Zheng, W., Thorne, N., Austin, C.P., Inglese, J., and Simeonov, A. (2008). A robotic platform for quantitative high-throughput screening. *Assay Drug Dev. Technol.* **6**:637 – 657. doi: http://dx.doi.org/10.1089/adt.2008.150.

[14] Eastwood, B.J., Farmen, M.W., Iversen, P.W., Craft, T.J., Smallwood, J.K., Garbison, K.E., Delapp, N.W., and Smith, G.F. (2006). The minimum significant ratio: a statistical parameter to characterize the reproducibility of potency estimates from concentration-response assays and estimation by replicate-experiment studies. *J. Biomol. Screen.* **11**:253 – 261. doi: http://dx.doi.org/10.1177/1087057105285611.

[15] Iversen, P.W., Eastwood, B.J., Sittampalam, G.S., and Cox, K.L. (2006). A comparison of assay performance measures in screening assays: signal window, Z' factor, and assay variability ratio. *J. Biomol. Screen.* **11**:247 – 252. doi: http://dx.doi.org/10.1177/1087057105285610

[16] Hill, A.V. (1910). The possible effects of the aggregation of the molecules of haemoglobin on its dissociation curves. *Journal of Physiology* **40**:4 – 7.

[17] Motulsky, H., Christopoulos, A. (2004). Fitting models to biological data using linear and nonlinear regression: a practical guide to curve fitting (New York: Oxford University Press).

[18] Weiss, J.N. (1997). The Hill equation revisited: uses and misuses. *FASEB J.* **11**:835 – 841.

[19] Southall, N.T., Jadhav, A., Huang, R., Nguyen, T., and Wang, Y. (2009). Enabling the Large Scale Analysis of Quantitative High Throughput Screening Data. In Handbook of Drug Screening. Second Edition, Seethala, R., Zhang, L. Eds. (New York: Taylor and Francis), pp. 442 – 462.

[20] Shukla, S.J., Nguyen, D.T., Macarthur, R., Simeonov, A., Frazee, W.J., Hallis, T.M., Marks, B.D., Singh, U., Eliason, H.C., Printen, J., Austin, C.P., Inglese, J., and Auld, D.S. (2009). Identification of pregnane X receptor ligands using time-resolved fluorescence resonance energy transfer and quantitative high-throughput screening. *Assay Drug Dev. Technol.* **7**:143 – 169. doi: http://dx.doi.org/10.1089/adt.2009.193.

[21] Hofmeyr, J.S., and Cornish-Bowden, A. (2000). Regulating the cellular economy of supply and demand. *FEBS Lett.* **476**:47 – 51.
doi: http://dx.doi.org/10.1016/S0014-5793(00)01668-9.

[22] Feron, O. (2009). Pyruvate into lactate and back: from the Warburg effect to symbiotic energy fuel exchange in cancer cells. *Radiother. Oncol.* **92**:329 – 333.
doi: http://dx.doi.org/10.1016/j.radonc.2009.06.025.

[23] Warburg, O. (1956). On respiratory impairment in cancer cells. *Science* **124**:269 – 270.

[24] Warburg, O. (1956). On the origin of cancer cells. *Science* **123**:309 – 314.
doi: http://dx.doi.org/10.1126/science.123.3191.309.

[25] Van der Heiden, M.G., Cantley, L.C., and Thompson, C.B. (2009). Understanding the Warburg effect: the metabolic requirements of cell proliferation. *Science* **324**:1029 – 1033.
doi: http://dx.doi.org/10.1126/science.1160809.

[26] Christofk, H.R., Van der Heiden, M.G., Harris, M.H., Ramanathan, A., Gerszten, R.E., Wei, R., Fleming, M.D., Schreiber, S.L., and Cantley, L.C. (2008). The M2 splice isoform of pyruvate kinase is important for cancer metabolism and tumour growth. *Nature* **452**:230 – 233.
doi: http://dx.doi.org/10.1038/nature06734.

[27] Christofk, H.R., Van der Heiden, M.G., Wu, N., Asara, J.M., and Cantley, L.C. (2008). Pyruvate kinase M2 is a phosphotyrosine-binding protein. *Nature* **452**:181 – 186.

[28] Noguchi, T., Inoue, H., and Tanaka, T. (1986). The M1- and M2-type isozymes of rat pyruvate kinase are produced from the same gene by alternative RNA splicing. *J. Biol. Chem.* **261**:13807 – 13812.
doi: http://dx.doi.org/10.1038/nature06667.

[29] Noguchi, T., Yamada, K., Inoue, H., Matsuda, T., and Tanaka, T. (1987). The L- and R-type isozymes of rat pyruvate kinase are produced from a single gene by use of different promoters. *J. Biol. Chem.* **262**:14366 – 14371.

[30] Dombrauckas, J.D., Santarsiero, B.D., and Mesecar, A.D. (2005). Structural basis for tumor pyruvate kinase M2 allosteric regulation and catalysis. *Biochemistry* **44**:9417 – 9429.
doi: http://dx.doi.org/10.1021/bi0474923.

[31] Yamada, K., and Noguchi, T. (1999). Regulation of pyruvate kinase M gene expression. *Biochem. Biophys. Res. Commun.* **256**:257 – 262.
doi: http://dx.doi.org/10.1006/bbrc.1999.0228.

[32] DeBerardinis, R.J., Lum, J.J., Hatzivassiliou, G., and Thompson, C.B. (2008). The biology of cancer: metabolic reprogramming fuels cell growth and proliferation. *Cell Metab.* **7**:11 – 20.
doi: http://dx.doi.org/10.1016/j.cmet.2007.10.002.

[33] Deberardinis, R.J., Sayed, N., Ditsworth, D., and Thompson, C.B. (2008). Brick by brick: metabolism and tumor cell growth. *Curr. Opin. Genet. Dev.* **18**:54 – 61.
doi: http://dx.doi.org/10.1016/j.gde.2008.02.003.

[34] Boxer, M.B., Jiang, J.-K., Van der Heiden, M.G., Shen, M., Skoumbourdis, A.P., Southall, N., Veith, H., Leister, W., Austin, C.P., Park, H.W., Inglese, J., Cantley, L.C., Auld, D.S., Thomas, C.J. (2009) Activators of the Tumor Cell Specific M2 Isoform of Pyruvate Kinase. Part 1: Substituted *N*,*N*′-Diarylsulfonamides. *J. Med. Chem*. **53**:1048 – 1055.
doi: http://dx.doi.org/10.1021/jm901577g.

[35] Auld, D.S., Southall, N.T., Jadhav, A., Johnson, R.L., Diller, D.J., Simeonov, A., Austin, C.P., and Inglese, J. (2008). Characterization of chemical libraries for luciferase inhibitory activity. *J. Med. Chem.* **51**:2372 – 2386.
doi: http://dx.doi.org/10.1021/jm701302v.

[36] Fan, F., and Wood, K.V. (2007). Bioluminescent assays for high-throughput screening. *Assay Drug Dev. Technol.* **5**:127 – 136.
doi: http://dx.doi.org/10.1089/adt.2006.053.

[37] Thompson, P.A., Wang, S., Howett, L.J., Wang, M.M., Patel, R., Averill, A., Showalter, R.E., Li, B., and Appleman, J.R. (2008). Identification of ligand binding by protein stabilization: comparison of ATLAS with biophysical and enzymatic methods. *Assay Drug Dev. Technol.* **6**:69 – 81.
doi: http://dx.doi.org/10.1089/adt.2007.100.

[38] Auld, D.S., Thorne, N., Maguire, W.F., and Inglese, J. (2009). Mechanism of PTC 124 activity in cell-based luciferase assays of nonsense codon suppression. *Proc. Natl. Acad. Sci. U.S.A.* **106**:3585 – 3590.
doi: http://dx.doi.org/10.1073/pnas.0813345106.

[39] Auld, D.S., Thorne, N., Nguyen, D.T., and Inglese, J. (2008). A specific mechanism for nonspecific activation in reporter-gene assays. *ACS Chem. Biol.* **3**:463 – 470.
doi: http://dx.doi.org/10.1021/cb8000793.

[40] Du, M., Liu, X., Welch, E.M., Hirawat, S., Peltz, S.W., and Bedwell, D.M. (2008). PTC 124 is an orally bioavailable compound that promotes suppression of the human CFTR-G542X nonsense allele in a CF mouse model. *Proc. Natl. Acad. Sci. U.S.A.* **105**:2064 – 2069.
doi: http://dx.doi.org/10.1073/pnas.0711795105.

[41] Kerem, E., Hirawat, S., Armoni, S., Yaakov, Y., Shoseyov, D., Cohen, M., Nissim-Rafinia, M., Blau, H., Rivlin, J., Aviram, M., Elfring, G.L., Northcutt, V.J., Miller, L.L., Kerem, B., and Wilschanski, M. (2008). Effectiveness of PTC 124 treatment of cystic fibrosis caused by nonsense mutations: a prospective phase II trial. *Lancet* **372**:719 – 727.
doi: http://dx.doi.org/10.1016/S0140-6736(08)61168-X.

[42] Welch, E.M., Barton, E.R., Zhuo, J., Tomizawa, Y., Friesen, W.J., Trifillis, P., Paushkin, S., Patel, M., Trotta, C.R., Hwang, S., Wilde, R.G., Karp, G., Takasugi, J., Chen, G., Jones, S., Ren, H., Moon, Y.C., Corson, D., Turpoff, A.A., Campbell, J.A., Conn, M.M., Khan, A., Almstead, N.G., Hedrick, J., Mollin, A., Risher, N., Weetall, M., Yeh, S., Branstrom, A.A., Colacino, J.M., Babiak, J., Ju, W.D., Hirawat, S., Northcutt, V.J., Miller, L.L., Spatrick, P., He, F., Kawana, M., Feng, H., Jacobson, A., Peltz, S.W., and Sweeney, H.L. (2007). PTC 124 targets genetic disorders caused by nonsense mutations. *Nature* **447**:87 – 91.
doi: http://dx.doi.org/10.1038/nature05756.

[43] Lyssiotis, C.A., Foreman, R.K., Staerk, J., Garcia, M., Mathur, D., Markoulaki, S., Hanna, J., Lairson, L.L., Charette, B.D., Bouchez, L.C., Bollong, M., Kunick, C., Brinker, A., Cho, C.Y., Schultz, P.G., and Jaenisch, R. (2009). Reprogramming of murine fibroblasts to induced pluripotent stem cells with chemical complementation of Klf4. *Proc. Natl. Acad. Sci. U.S.A.* **106**:8912 – 8917.
doi: http://dx.doi.org/10.1073/pnas. 0903860106.

[44] Inglese, J., Thorne, N., and Auld, D.S. (2009). Reply to Peltz et al: Post-translational stabilization of the firefly luciferase reporter by PTC 124 (Ataluren). *Proc. Natl. Acad. Sci. U.S.A.* **106**:E65.
doi: http://dx.doi.org/10.1073/pnas.0905457106.

[45] Peltz, S.W., Welch, E.M., Jacobson, A., Trotta, C.R., Naryshkin, N., Sweeney, H.L., and Bedwel, D.M. (2009). Nonsense suppression activity of PTC 124 (ataluren). *Proc. Natl. Acad. Sci. U.S.A.* **106**:E64.
doi: http://dx.doi.org/10.1073/pnas.0901936106.

[46] Inglese, J., Johnson, R.L., Simeonov, A., Xia, M., Zheng, W., Austin, C.P., and Auld, D.S. (2007). High-throughput screening assays for the identification of chemical probes. *Nat. Chem. Biol.* **3**:466.
doi: http://dx.doi.org/10.1038/nchembio.2007.17.

[47] Cleveland, P.H., and Koutz, P.J. (2005). Nanoliter dispensing for uHTS using pin tools. *Assay Drug Dev. Technol.* **3**:213 – 225.
doi: http://dx.doi.org/10.1089/adt.2005.3.213.

[48] Auld, D.S., Zhang, Y.Q., Southall, N.T., Rai, G., Landsman, M., Maclure, J., Langevin, D., Thomas, C.J., Austin, C.P., and Inglese, J. (2009). A Basis for Reduced Chemical Library Inhibition of Firefly Luciferase Obtained from Directed Evolution. *J. Med. Chem.* **52**:1450 – 1458.
doi: http://dx.doi.org/10.1021/jm8014525.